AD_____

Award Number: W81XWH-04-1-0677

TITLE: Nanoprobe Directed Tumor Imaging Using pH Activated Peptides as Contrast Agent Carriers

PRINCIPAL INVESTIGATOR: John E. Mata, Ph.D.
Scout Gustafson, D.V.M.

CONTRACTING ORGANIZATION: Oregon State University
Corvallis, OR 97331

REPORT DATE: March 2006

TYPE OF REPORT: Final

PREPARED FOR: U.S. Army Medical Research and Materiel Command
Fort Detrick, Maryland 21702-5012

REPORT DOCUMENTATION PAGE

Form Approved
OMB No. 0704-0188

1. REPORT DATE *(DD-MM-YYYY)*	**2. REPORT TYPE**	**3. DATES COVERED** *(From - To)*
01-03-2006	Final	15 Aug 2004 – 14 Feb 2006

4. TITLE AND SUBTITLE
Nanoprobe Directed Tumor Imaging Using pH Activated Peptides as Contrast Agent Carriers

5a. CONTRACT NUMBER

5b. GRANT NUMBER
W81XWH-04-1-0677

5c. PROGRAM ELEMENT NUMBER

6. AUTHOR(S)
John E. Mata, Ph.D.
Scout Gustafson, D.V.M.

E-mail: john.mata@oregonstate.edu

5d. PROJECT NUMBER

5e. TASK NUMBER

5f. WORK UNIT NUMBER

7. PERFORMING ORGANIZATION NAME(S) AND ADDRESS(ES)
Oregon State University
Corvallis, OR 97331

8. PERFORMING ORGANIZATION REPORT NUMBER

9. SPONSORING / MONITORING AGENCY NAME(S) AND ADDRESS(ES)
U.S. Army Medical Research and Materiel Command
Fort Detrick, Maryland 21702-5012

10. SPONSOR/MONITOR'S ACRONYM(S)

11. SPONSOR/MONITOR'S REPORT NUMBER(S)

12. DISTRIBUTION / AVAILABILITY STATEMENT
Approved for Public Release; Distribution Unlimited

13. SUPPLEMENTARY NOTES

14. ABSTRACT

We characterized a class of modified peptides designed to activate in the extracellular space of tumors in which pH is below 7.0 in cell culture and in tumor bearing mice. These "molecular engines" change shape in a low pH environment, become lipophilic, and embed into the plasma membrane. Our studies suggest that a molecular engine with a pT of 6.8-6.9 will deliver an 8-carboxyfluoroscein ligand to the surface of tumor cells in C57blk-J6 mice bearing subcutaneously transplanted Lewis lung cell-derived tumors following an iv injection of 27 nmoles (0.1 mg) peptide with FITC-labeled ligand. These observations were confirmed by flow cytometric analysis. Proof of principle for their diagnostic utility of this technology was obtained by injection of a 99mTc labeled peptide followed by gamma scintigraphy. This technology has tremendous potential for highly specific medical intervention at the molecular scale.

15. SUBJECT TERMS
Nanotechnology, scintography, nuclear medicine, peptide

16. SECURITY CLASSIFICATION OF:			**17. LIMITATION OF ABSTRACT**	**18. NUMBER OF PAGES**	**19a. NAME OF RESPONSIBLE PERSON**
a. REPORT	**b. ABSTRACT**	**c. THIS PAGE**			USAMRMC
U	U	U	UU	13	**19b. TELEPHONE NUMBER** *(include area code)*

Table of Contents

INTRODUCTION

Early detection of breast cancer may benefit from peptide based probes capable of activating and embedding into the acid regions of tumors. Tumors have been widely recognized to have an extracellular pH which is significantly lower that normal tissue(*1-11*). The core nanotechnology of the diagnostic drug delivery system being investigated is a class of modified peptides designed to activate in the extracellular space of tumors in which pH is below 7.0. These "molecular engines" change shape in a low pH environment, become lipophilic, and embed into the plasma membrane. Little is known about this technology. Therefore, we tested the central hypothesis that pH activated peptides attached to an appropriate contrast agent could be used to detect tumors for diagnosis of breast cancer and other solid tumors. The development of nanotechnology for diagnostic and thereapeutic approaches to cancer treatment will have a broad impact in areas of human and veterinary oncology. The technology that we are currently developing is a platform technology that we can use to delivery a variety of small molecules to areas of low pH. We envision that we can take this research beyond diagnostics into treatment paradigms for cancer, wound healing, regenerative medicine, and provide research tools to measure changes in pH within the body.

BODY

Our research began with *in vitro* studies to characterize the peptides in Lewis lung carcinoma cells (LLC1) under different peptide designs, peptide concentration, and pH conditions. Two peptide lengths were tested in cell culture and *in vivo* following initial testing of 23 permutations of the final selected peptides at GeneTools, LLC.

Task 1. **To determine the sensitivity and limit of detection of Lewis lung carcinoma cells (LLC1) and MCF-7 breast carcinoma cells with activated peptide conjugated to a fluoroscein isothiocyanate (FITC) ligand or a technicium (^{99}Tc) containing chelator ligand. (months 1-3)**

a. Perform a dose response curve with a series of peptides containing FITC ligands at an activating pH to determine the % dose retained in the cell pellet following several washes.
b. Perform a pH titration with an optimal dose to determine the effective target pH for a series of engines.

The use of pH activated peptides as contrast agent carriers require sufficient uptake onto the surface of

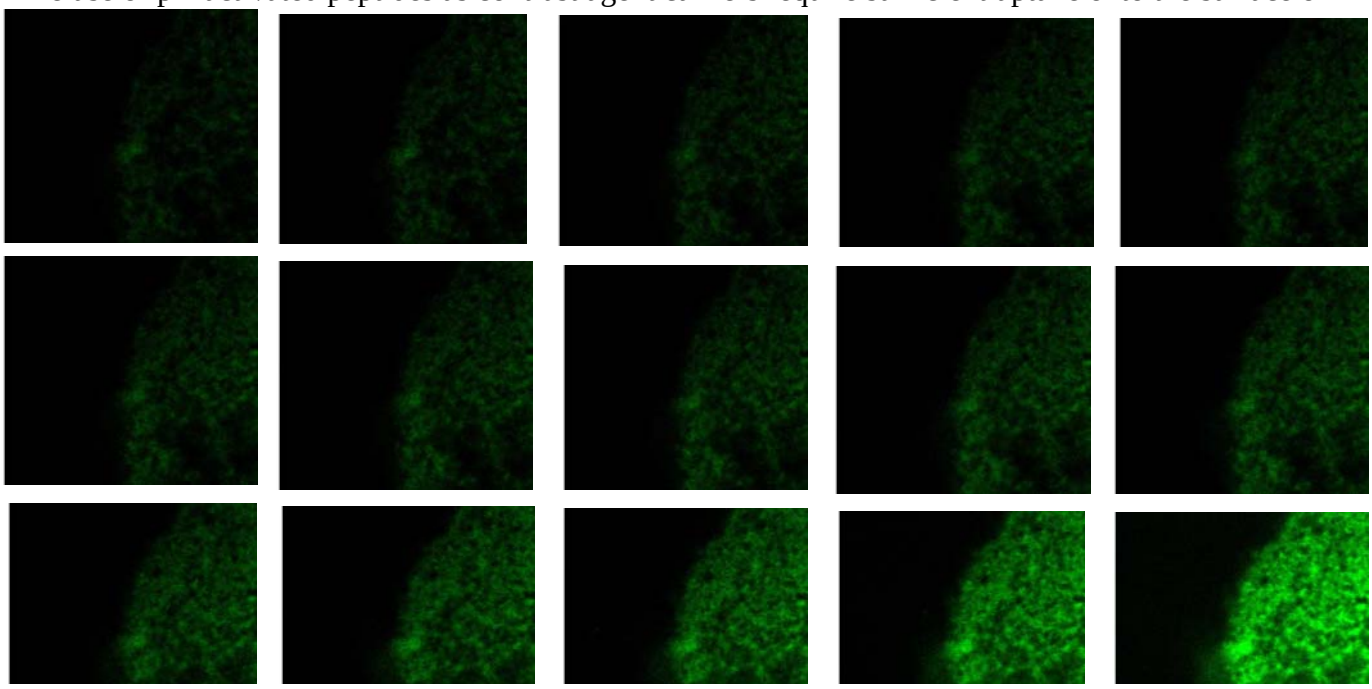

Figure 1. Time lapse confocal imaging of peptide accumulation on the surface of LLC1 cells in culture. Top left is 5 minutes with time points at each minute (from left to right) to 15 minutes at bottom right.

cancer cells to provide a low signal to noise ratio. Studies were conducted to evaluate the ability of activated fluorescently labeled peptide to accumulate over a short period of exposure onto the surface of Lewis Lung carcinoma cells in culture. Upon acidification of the media to 6.5by titration with HCl and under confocal microscopy using a 100X objective, we observed and measured the fluorescence associated with the cell membrane at 10 second intervals for a total of 8.0 minutes (Figure 1). Each individual scan

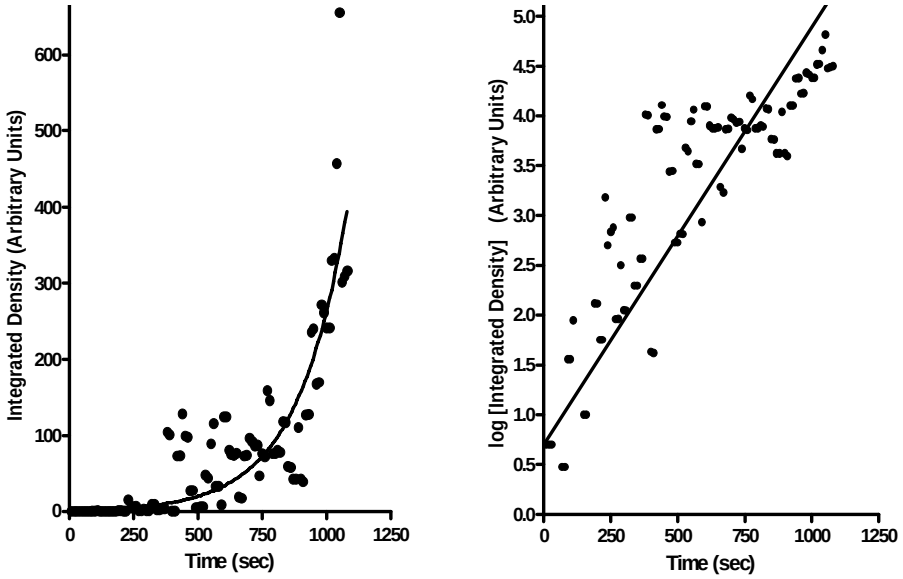

Figure 2. Analysis of fluorescence intensity of cell surface during peptide accumulation after activation of peptide at pH 6.5. Analysis was performed with Scion Image (Beta 4.0.2, Scion Corp., Frederick, Md)

was analyzed as a digital image using Scion Image software Beta 4.0.2 (Scion Corp., Frederick, Maryland) and the results of integrated density analysis of the cell surface is presented in Figure 2. Our analysis demonstrates a nearly 5.0 log increase in intensity over an 8 minute period. However, it is important to recognize that this increase does not take into account the substantial bleaching of the 8-carboxyfluoroscein derived signal that occurs with each scan of the laser and our analysis may underestimate the increase in signal by several logs.

The bleaching and general instability of the 8-carboxyfluoroscein ligand proved to be problematic for other aspects of our analysis. We were able to develop a method for the extraction of the peptide from tissues and blood. However, the signal-to-noise ration of the control tissues relative to the peptide was erratic and new methods are currently being developed that will use a near-infared emitting flourochrome. These fluorochromes fluoresce in a range that will separate the autofluorescence from tissue samples from the signal in the near IR. These peptides are currently in development and will be employed as the project continues.

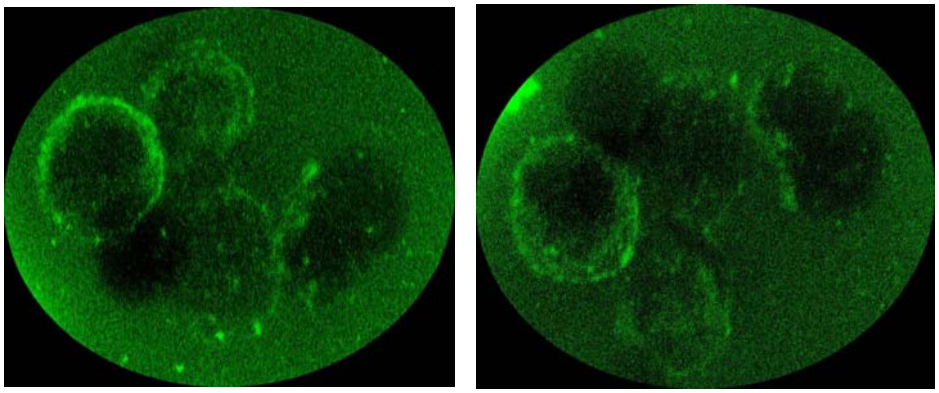

Figure 3. Three dimensional images showing peptide embedded on the surface of Lewis lung carcinoma cells in culture.

A three dimensional reconstruction using confocal imaging presented in figure 3 reveals that the peptide is present on the cell surface and has not accumulated to any appreciable degree within the cell. This observation provides evidence that our peptides are properly engineered to deliver a payload to the surface of the cell and confirms that a 22 amino acid chain is sufficient to allow accumulation of the peptide on the cell surface without passing through the membrane.

We performed a pH titration on peptides 1 and 2 at a concentration that provided approximately 10.0 fluorescent units at an activating pH. Binding of peptide 2 to the cells occurred at the range of pH's tested indicating that this molecule was too lipophillic to be useful in our model. The results of pH titration on binding to LLC1 cells is presented in Figure 4. As can be seen in this figure, the transition from lipophyllic interactions to hydrophillicity and low cell binding occurs between pH 7.0 and 7.2 with a Hillslope of -16.13 ± 14.23. The high standard error is most likely due to the limited number of observations within the peptide transition pH range and the variability within the data sets. The significant bleaching of FITC under the polarized light sources used to image and the variability of data from binding experiments have led us to conclude that the 8-carboxy-fluoroscein labeled peptides are not as useful a research tool as we had anticipated. However, these compounds proved to be useful for some imaging, qualitative characterizations of distribution, and flow cytometric analysis *in vivo*. Experiments to conjugate a near infared (NIR) fluorescent dye to the peptide are currentliy underway and we expect that the use of (NIR) dyes will provide lower background and increase the signal to noise ratio.

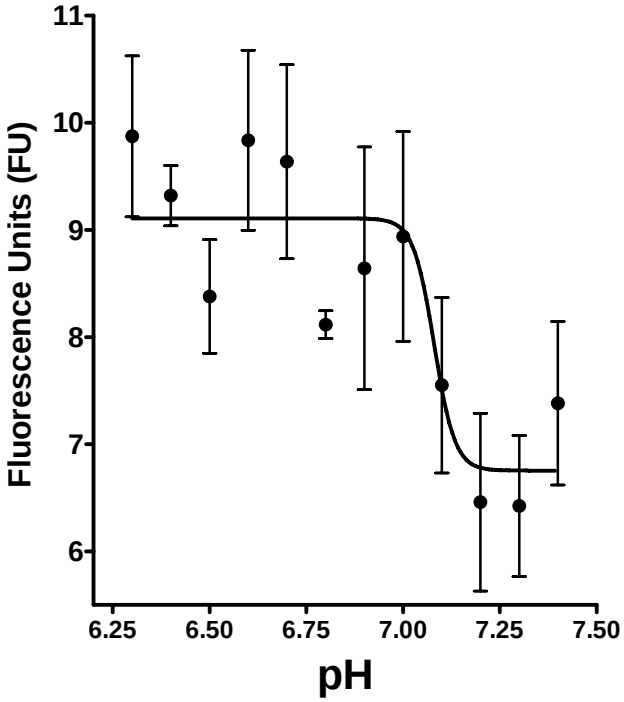

Figure 4. Effects of pH transition from acidic to physiologic pH on the binding affinity of FITC-labeled peptide for LLC1 cells in culture.

c. Evaluation of conditions for optimal ^{99}Tc chelation and isolation of chelate.

Optimization of conditions for 99Tc chelation and isolation of chelate began with the synthesis of peptides containing an attached chelator moiety. Initially, our collaborator, GeneTools, LLC tried to construct a tri-dentate chelator capable of chelating ^{99}mTc based on the chelating properties of histindine(*12*). However, it was found that groups within the molecule that were essential for chelating properties could not be protected and synthesis of the chelator with the appropriate reactive group for linkage to the peptide was not readily achieved. Therefore, we chose to use the N-hydroxysuccinimide ester of S-acetyl mercaptoacetyltriglycine (MAG3) as the chelator moiety attached to the peptide. The protocol developed for these molecules are based on a similar labeling procedure described by Hnatowich *et al.*(*13*).

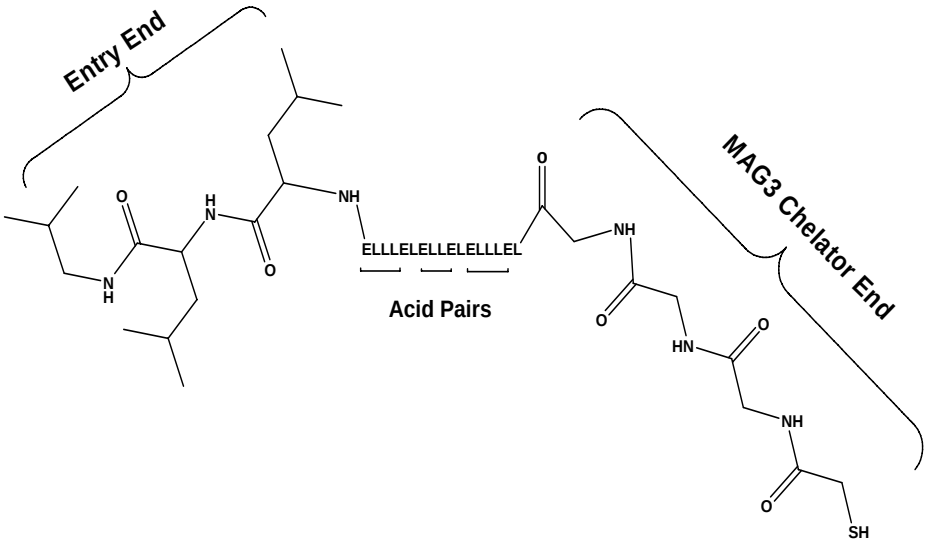

Figure 5. Drawing of the chemical structure of peptide 1 conjugated to the MAG3 chelator functional group.

A series of peptides was prepared and initially tested at GeneTools, LLC. They provided us with two peptides suitable for use with the ^{99}mTc.

These peptides differed in pH of transition (pT) with Peptide 1 having a pT between 7.0 and 7.2 and Peptide 2 a pT of 7.2-7.4. These peptides contain an entry end which allows the peptide to initiate entry into the cell membrane and the delivery end which can be functionalized with a variety of ligands for use as a diagnostic tool or therapeutic drug delivery device.

d. Repeat steps a and b with a series of peptides conjugated to a technicium chelated ligand.
e. Determine the relative signal to noise ratio of activated peptide compared to control treatment for the ^{99}Tc labeled peptide.

In conducting these tasks it became immediately apparent that the specific activity of the peptides was very high and efficiency of ^{99}mTc chelation was nearly complete.

Task 2. **To characterize the *in vivo* distribution of FITC-labeled and technicium containing pH sensitive peptides in a mouse model of primary tumor and lung metastatic disease. (months 3-6)**

a. Perform pharmacokinetic analysis of FITC-labeled peptide in LLC1 transplanted tumor bearing mouse.

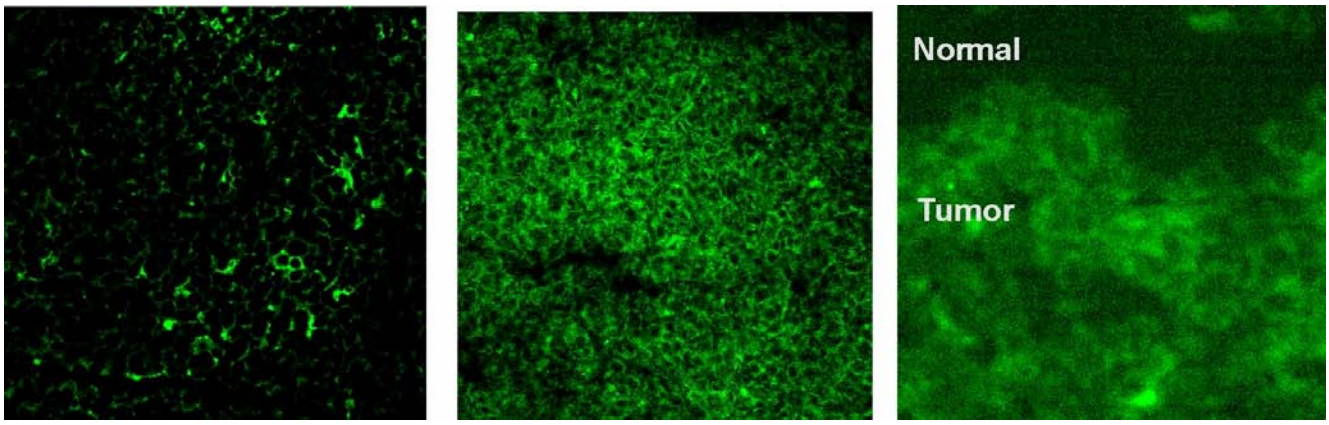

Figure 6. Confocal image of a Lewis lung cell-derived tumor from a mouse treated with saline (left panel) and molecular engine peptide with FITC as a fluorescent ligand demonstrating accumulation of peptide in tumor tissue (center panel). Fluorescence image of transition from tumor to connective tissue (right panel)

A limited data set was generated using the FITC-labeled peptide to characterize *in vivo* distribution of these molecules in mice. In mice injected with peptide or saline control, it was evident by confocal microscopy and by fluorescent microscopy that there was a significant increase in fluorescence within the transplanted tumor 2.0 hours following injection of 27 nmoles of peptide into the tail vein (Figure 6, left and center). Additionally,

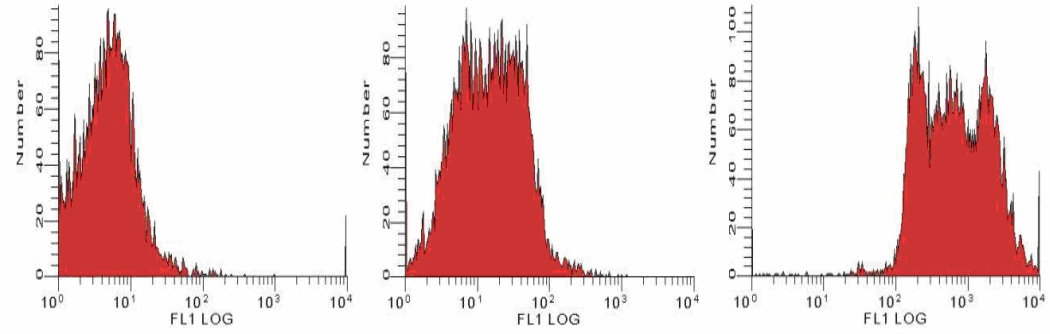

Figure 7. Flow cytometric analysis of tumor cells collected from Lewis lung tumor transplants in C57Blk-J6 mice. Left panel shows the background fluorescence of tumor cells from a saline treated animal 2 hours post-injection. Center panel is the analysis of the cells in panel 1 treated with 0.004 mg/ml peptide ex-vivo in PBS at pH 6.5. Right panel is the analysis of cells excised from the tumor of a mouse treated with a single iv injection of 0.1 mg (27 nmoles) 8-carboxyfluoroscein labeled peptide and collected from the transplanted tumor 2 hours post injection.

tumor margin was visualized and revealed a clear distinction between tumor and adjacent normal connective tissue.

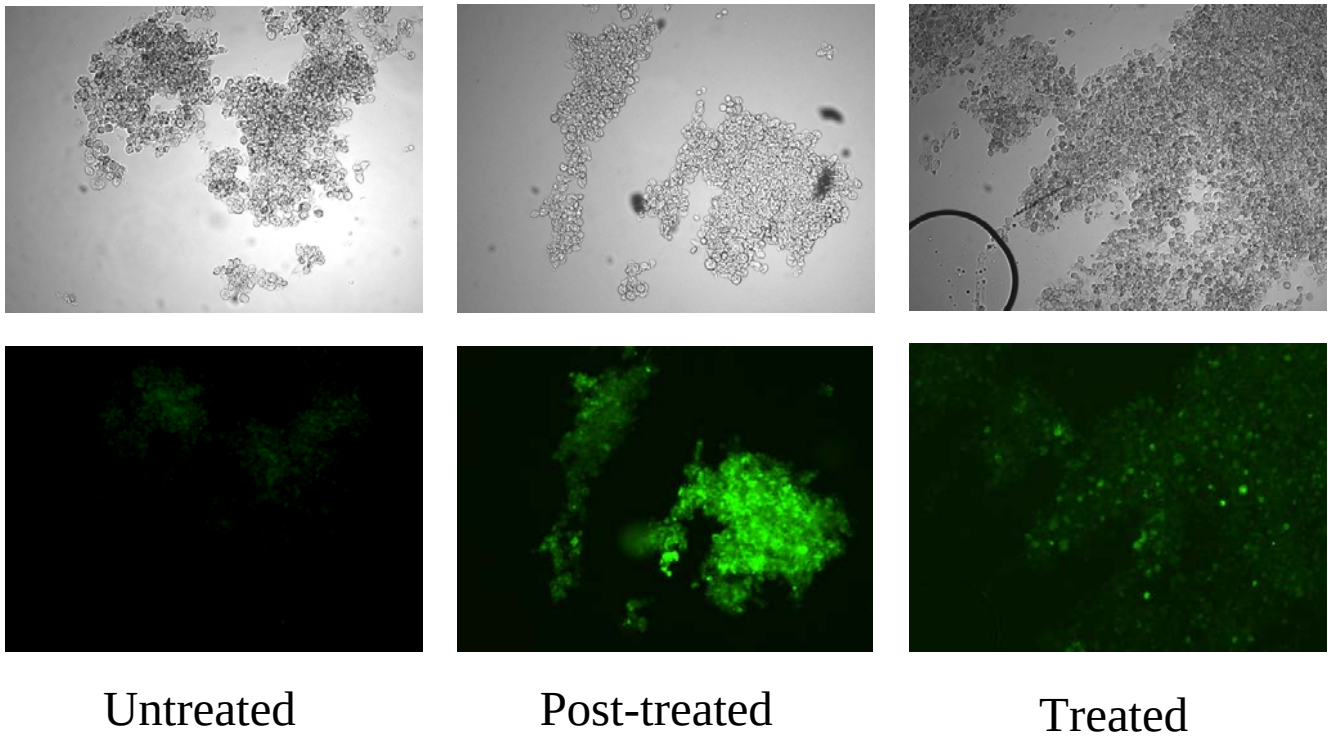

Figure 8. Confocal microscopy of cells collected from Lewis lung tumor transplants in C57Blk-J6 mice. Right column are photomicrographs of tumor cells collected from control animals and visualized by bright field (top) and fluorescence (bottom). Center panels are cells from the same tumor presented on the left that has been incubated for 5 minutes in the presence of peptide at pH 6.5 and then washed with PBS (pH 7.4) before being fixed with 70% ethanol. Right panels are cells excised from the tumor of a representative mouse treated with a single iv injection of 0.1 mg (27 nmoles) 8-carboxyfluoroscein labeled peptide and collected from the transplanted tumor 2 hours post injection.

Tumors were disaggregated, fixed with 70% ethanol, analyzed by flow cytometry and visualized under confocal microscopy. Flow cytometry results presented in Figure 7 demonstrate that two populations of cells are present in tumors of mice injected with FITC-labeled peptide. The two peaks present in the left panel of Figure 7 suggest that the peptide preferentially accumulates on the surface of a single population of cells. Presumably due to areas of low pH within the tumor which provide a medium suitable for activation of the tumor and areas of normal pH where blood flow provides a microenvironment not conductive to peptide activation.

This observation can be seen in Figure 8 with the same samples analyzed in Figure 7 when visualized under confocal microscopy. The right panel in Figure 8 clearly shows

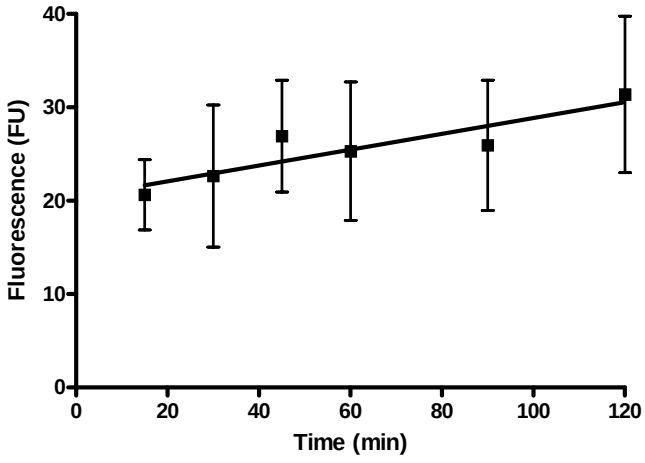

Figure 9. Plasma fluorescence from mice treated with a single iv injection of 0.1 mg (27 nmoles) 8-carboxyfluoroscein labeled peptide and collected by retro orbital vein puncture at 15, 30, 45, 60, 120 and 240 minutes post injection.

the variation in labeling of cells within the tumor cell population when observed under fluorescent confocal microscopy.

b. Analysis of Cp_{max} (plasma concentration maxima) and Tp_{max} (time of Cp_{max}) for FITC labeled peptides.

Plasma kinetics was attempted with the FITC-labeled peptide 1, however, the results were not satisfactory and background fluorescence from the plasma was higher than we had anticipated. We have included a graph of the plasma concentrations in mice in Figure 9. When proposing this aim we had anticipated a short but significant distribution phase following injection of the contrast agent into the tail vein. We hypothesized that the accumulation of peptide within the tumor will be a function of blood flow through the tumor and the elimination rate constant following iv injection. Because the plasma autofluorescence is unacceptably high, we are designing a peptide with a near infared dye which should allow us to increase the signal to noise ratio in our analysis. Additionally, we have chosen to follow the distribution and total amount of the drug through the use of ^{99}mTc labeled peptide. Both peptide 1 and peptide 2 were used initially, however, peptide 2 was a failure in our system due to a high affinity for tissue at the site of injection and the liver. Because peptide 2 was not useful in our model, the data that we present is from peptide 1. Figure 10 shows the gamma radiation from a mouse injected with 99mTc via tail vein. Radioactivity leaves the site of injection and appears to accumulate primarily in the stomach and thymus. No radioactivity is detected in tumor. In contrast, tumor bearing mice retain radioactivity at the site of

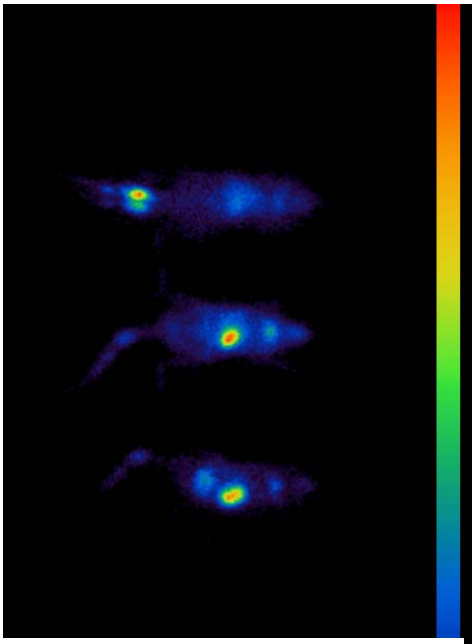

Figure 10. Scintigraphic photo of mice injected with 99mTc.

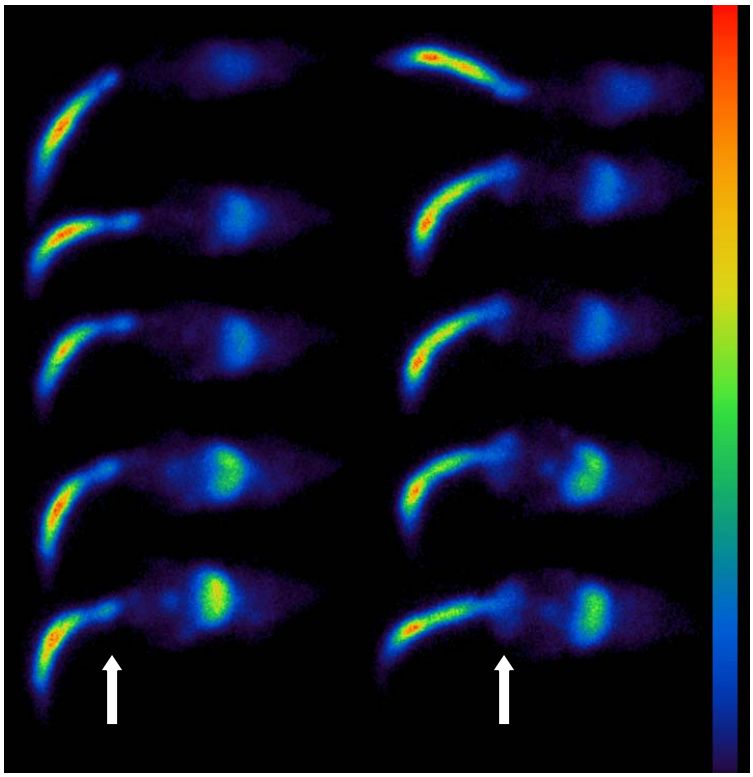

99mTc labeled peptide and imaged at 0, 2, 4, 8, and 24 hours top to bottom. Mice have a small (left) and large tumor (right) at the base of the tail.

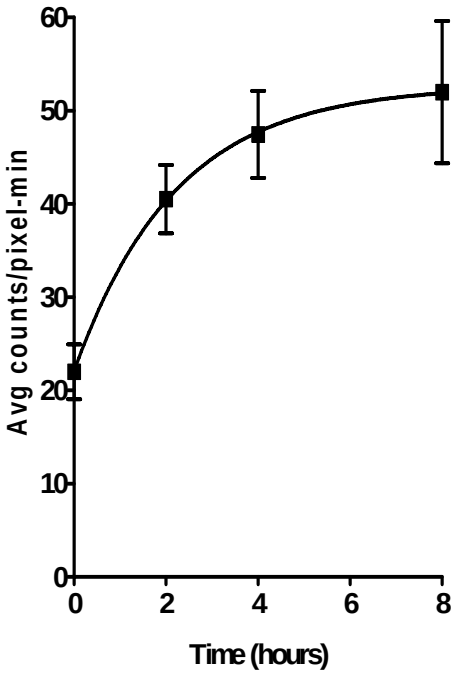

Figure 12. Scintigraphic analysis of peptide accumulation in lung and liver area following injection of 99mTc. (n=8)

injection, in lungs, liver, and tumors Figure 11. The mice presented in Figure 11 are representative of the observations of mice injected with 99mTc peptide and visualized by scintigraphy. While we achieved our overall objective of using this novel technology to image tumors, we felt the retention of peptide at the site of injection and in the lungs and liver were cause for concern that the peptide may be aggregating due to intermolecular interactions. Analysis of the peptide in the lungs and liver reveals steady accumulation of peptide in the lungs and liver suggesting that peptide may be slowly entering circulation from the site of injection (Figure 12) . While the tail vein injections of LLC1 cells often produce metastatic lesions, the radioactivity in the lung could not be attributed to nodules in the lung. We became concerned that the retention of peptide in the lung may be from intermolecular interactions between peptides. In order to prevent aggregation of peptides within the peptide formulation, we reformulated the peptide following the chelation reaction by adding 1/3 volume of 900 mM Mannitol. We reason that we will be able to analyze the entire body of the animal and estimate a C_{max} for individual organs or tumors based on these data points. Scintigraphic analysis of tumor bearing animals injected via tail vein with 99mTc revealed that peptide is excreted by the kidney (Figure 13). Drug can be visualized in the major organs and is evident in systemic circulation, liver, lungs, kidney, bladder and tumor at two hours. At four hours, the peptide is compartmentalized to the liver and tumor. This change in peptide distribution suggests an alpha and beta phase elimination. The peptide present in systemic circulation can be seen at the 2 hour time point and we infer that the alpha phase is rapid and that beta elimination begins between 2 and 4 hours. The drug remains in the liver and tumor for an extended period and can be visualized at 24 hours. We speculate that the accumulation in the liver is due to the leucines present in the entry end of the peptide and that modifications to this end of the peptide may abrogate liver uptake. Modifications to the peptide to test this hypothesis are ongoing.

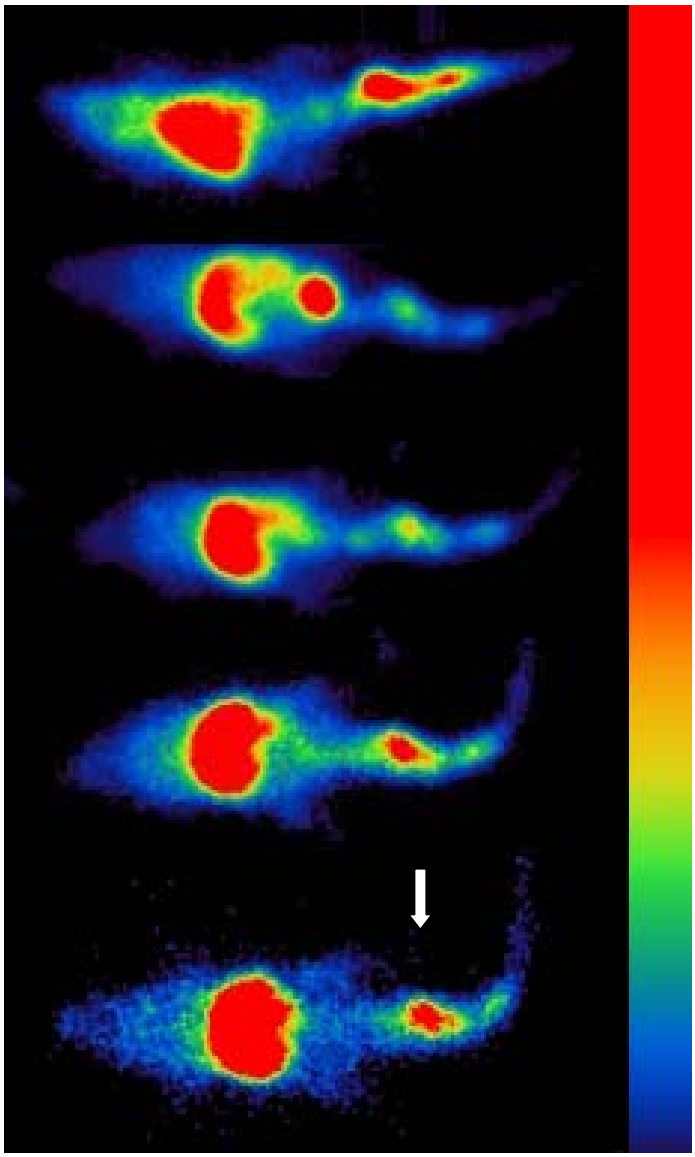

Figure 13. Technicium imaging *in vivo*. Scintigraphy was performed at the time of injection, and 2, 4, 8 and 24 hours following injection (top to bottom, respectively). Acquisition time was increased at each timepoint to appoximate the rate of decay of the 99Tc. This mouse has a small tumor at the base of the tail (arrow). Unconjugated 99Tc demonstrates markedly different biodistribution (data not shown).

c. **Analysis of tissue distribution and maximum fluorescence in tumors.** A total of 4 tumor bearing animals per group were used to determine tissue distribution and maximum fluorescence in tumors (4 control, 4 treated with two peptides), with each experiment repeated for a total of 8 animals per group. Peptide was extracted from tissues and analyzed in a 96-well flourospectrometer for total intensity. The data collected suffered from a high background and control samples were not significantly different from treatment groups for any tissues measured due to the high background values at the wavelengths of FITC emission. Because of the fluorescent background at the emission wavelength of the FITC-labeled peptide, we conjugated the pepitide to a near-IR fluorescent

dye (Alexafluor 680). Following conjugation and purification we found that our peptide was highly fluorescent as 700 nm and retained some signal at 800. This finding was significant because heme containing components in the blood and other tissues are fluorescent at the 700 emission wavelength. We have performed preliminary experiments with these near-IR probes in tumor bearing mice. Our results indicate the near-IR probes may have utility for future work with these peptides. Although heme interferes with the signal at the 700 channel. The signal at 800 nm has sufficiently low background that near-IR analysis for plasma kinetics and tumor distribution may be feasible. Figure 14 shows the results of a pilot study with the near IR-fluorochrome labeled peptide. As seen in the image, the peptide treated mouse has increased fluorescence in the tumor at 2 hours compared to the adjacent tissue. A similar tumor from an animal treated identically and euthanized at time 0 is provided for comparison. Although we have tested this approach to tumor imaging in only a few mice at the writing of this report due to the small quantity of labeled dye that was prepared, the near-infared probes appear to be useful in the 800 nm range. The tumors are very apparent and tumor margins are evident in the tumors from peptide treated animals. Additional studies will be performed in order to evaluate this approach. Additionally, we will conjugate larger quantities of peptides with near-IR probes with emission spectra in the 750 nm range. We anticipate that these molecules will have higher fluorescence at the 800 nm wavelength and provide higher contrast at lower dosages.

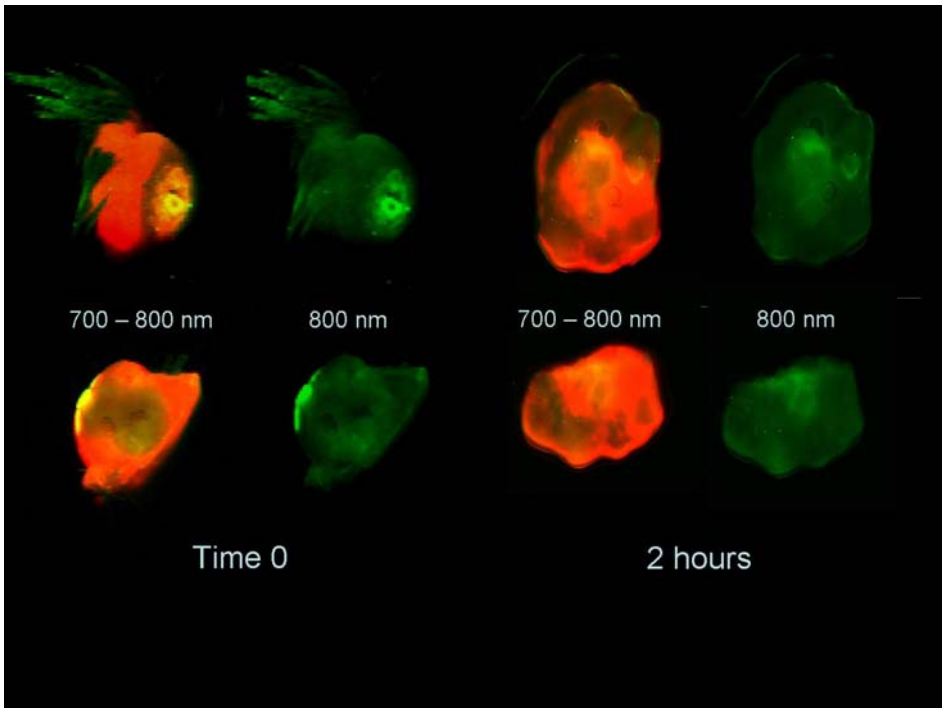

Figure 14. Near-IR image of tumors from animals injected with approximately 0.1 mg (2.7 nmoles) of Alexafluor 680 conjugated peptide and imaged at 0 and 2 hours. Tumors from two representative animals are presented. The top row of images are of subcutaneously transplanted 0.5 cm LLC1 tumors. Bottom row of images are the same tumors in crossection. Bright fluorescence on the edge of the control tumor is due to a scaly necrotic region on the surface of the tumor.

d. Analysis of blood chemistry for signs of toxicity due to treatment. These peptides have not been administered to animals prior to our intital experiments and we carefully monitored animals for signs of acute toxic responses. The animals tolerated the iv injections well and there were no signs of adverse reaction to the injections. Plasma samples were collected up to 4 hours and blood chemistry was performed. The results of that analysis were unremarkable and not significantly different from control. This is not surprising at the short time frame of the experiment, however, while not a toxic event *sensu stricto,* a possible undesired effect of molecules is stimulation of a specific immune response or overt innate immune response. An anaphylactic response is possible and would be clinically identifiable shortly after injection of the drug. Through the short-term studies, we were able to determine that acute toxicity was not evident and this provided enough data to amend our animal use protocol to test longer time periods. Additionally, we have extended the time frame for our experiments to include longer time periods for the scintigraphic analysis. Although blood chemistry would be helpful for these experiments, because of the time required to decay the radioactivity in the samples and the increase in animal handling required, we chose to evaluate toxicity using histopathological techniques. Animals were necropsied at the end of each scintigraphic analysis and organs were placed in 10% buffered

formalin. We allowed the ^{99}mTc to decay to background level prior to submitting the tissues to the Veterinary Diagnostics Laboratory at Oregon State University. The results of this analysis suggests that there were minor anesthesia related effects of the procedure and some renal pathology that was consistent with the extent of disease progression in the animals. No findings of toxicity that could be attributed to the administration of the peptides.

Task 3. **To characterize the *in vivo* distribution of FITC labeled and technicium containing pH sensitive peptides in a mouse model of carcinoma of the breast. Months (5-12)** These tasks have yet to be completed. A grant extension has been requested and granted in order to complete the tasks outlined below.

a. Perform pharmacokinetic analysis of technicium chelated peptides in MCF-7 xenographed tumor bearing mouse.
b. Analysis of Cp_{max} and Tp_{max} for technicium labeled peptides.
c. Analysis of tissue distribution in the body and maximum signal in tumors.
d. Determine the sensitivity of the technique in the evaluation of metastic disease following resection of the primary mammary tumor.
e. Analysis of blood chemistry for signs of toxicity due to treatment.

KEY RESEARCH ACCOMPLISHMENTS

- We have successfully synthesized a pH activated peptide capable of targeting solid tumors and completed testing *in vitro* and in tumor bearing mice.
- We have developed peptides with a MAG3 chelator attached.
- We have developed the methodology to chelate ^{99}mTc.
- We have successfully imaged tumors in mice using pH activated peptides and gamma scintigraphy.
- We have refined the formulation of the peptide to optimize the labeling of tumors *in vivo*.
- During the course of the radionuclide imaging a Master of Science student was trained.
- We have successfully conjugated pH activated peptide to a near infared fluorescent dye.
- We have successfully imaged a tumor following injection of a near infared dye conjugated peptide.
- We have successfully identified a potential candidate for development of non-invasive detection of small tumors.

REPORTABLE OUTCOMES

We have successfully completed much of the proposed work and have made observations about pH activated peptides that are of interest to researchers in the field. We are currently preparing a manuscript to describe the results of our work and have presented many of our findings at several meetings including:

Mata, J., Gustafson, S., Loehr, C., Rodriguez-Proteau, R., Slauson, M., Summerton, J. (2005) Tumor targeting using pH activated molecular engines. Eleventh Annual Blood-Brain Barrier Disruption Consortium Meeting. Nanobiology and Nanomedicine in the Pacific Northwest. Abstract number 7.

Mata, J., Gustafson, S., Loehr, C., Rodriguez-Proteau, R., Slauson, M., Summerton, J. (2005) Nanoprobe directed tumor imagine using pH activated peptides as contrast agent carriers. Fourth Annual Era of Hope Department of Defense Breast Cancer Research Program Meeting. Abstract number P15-6.

Dyal, L.S., Mata, J.E., Gustafson S.B., Slauson, M.E., Summerton, J.E. and Löhr C.V. Molecular Engines: A new platform for cancer diagnosis and treatment. 22nd Annual meeting of PANWAT. Astoria, Oregon.

In addition to poster and platform presentations the important observations were used as preliminary data for the following grant applications:

Molecular engines: a platform technology for diagnosis and treatment of cancer NIH- National Cancer Institute, RO1 mechanism. Not funded.

Therapeutic Applications of pH-activated Molecular Engines In Vivo: A New Platform Nanomedical Technology for Treatment of Breast Cancer and Metastatic Disease. Idea Award for Breast Cancer Research, Department of Defense. Currently under review.

Nanomedicine in Cancer: pH Activated Molecular Engines. The Susan G. Komen Breast Cancer Foundation. Currently under review.

Molecular engines: a platform technology for diagnosis and treatment of cancer. RFA-CA-07-002 Title: Application of Emerging Technologies for Cancer Research. NIH – National Cancer Institute, R21 mechanism. Currently under review.

CONCLUSIONS

The development of tumor targeting molecules that rely on the physiological properties of tumors have been of interest in cancer drug and diagnostics development for several decades(*14*). The embedding peptide that we have developed in the course of this project is a novel approach to targeted delivery of medically useful molecules to tumors. Our studies, while not complete, indicate that this technology will have broad utility for targeting tumors for diagnosis and treatment of cancer. Through this grant, we have defined active molecules and developed methods that will guide the future development of this technology. Our proposed research was designed to evaluate this technology for use as a cancer diagnostic tool and our results support the continued development of these molecules for diagnostics. We are currently involved in studies to of peptides that are modified to increase the targeting ability to tumors. We believe that this will allow the delivery of therapeutic agents to tumors. We are currently conducting work outlined in Task 3 which will test this technology in a breast cancer model with our newly synthesized molecules. This work is not complete at the time of this report and if you should need additional information we can provide an amended Final report at a later date. We are confident that our technology will provide a method of identifying mammary tumors based on physiological parameters that are unique to tumors and are grateful for the opportunity to work with your program.

REFERENCES

1. Y. Tagashira, S. Takeda, K. Kawano, S. Amano, *Gan* **45**, 99 (Sep, 1954).
2. E. Svastova *et al.*, *FEBS Lett* **577**, 439 (Nov 19, 2004).
3. J. L. Wike-Hooley, J. Haveman, H. S. Reinhold, *Radiother Oncol* **2**, 343 (Dec, 1984).
4. J. L. Wike-Hooley, A. P. van den Berg, J. van der Zee, H. S. Reinhold, *Eur J Cancer Clin Oncol* **21**, 785 (Jul, 1985).
5. A. P. van den Berg, J. L. Wike-Hooley, A. E. van den Berg-Blok, J. van der Zee, H. S. Reinhold, *Eur J Cancer Clin Oncol* **18**, 457 (May, 1982).
6. S. R. Smith, R. D. Griffiths, P. A. Martin, R. H. Edwards, *Radiology* **173**, 572 (Nov, 1989).
7. P. A. Schornack, R. J. Gillies, *Neoplasia* **5**, 135 (Mar-Apr, 2003).
8. D. A. Rottenberg *et al.*, *Ann Neurol* **17**, 70 (Jan, 1985).
9. N. Raghunand *et al.*, *Biochem Pharmacol* **57**, 309 (Feb 1, 1999).
10. N. Raghunand, R. Martinez-Zaguilan, S. H. Wright, R. J. Gillies, *Biochem Pharmacol* **57**, 1047 (May 1, 1999).
11. N. Raghunand *et al.*, *Br J Cancer* **80**, 1005 (Jun, 1999).
12. A. Egli *et al.*, *J Nucl Med* **40**, 1913 (Nov, 1999).
13. D. J. Hnatowich, F. Chang, K. Lei, T. Qu, M. Rusckowski, *Appl Radiat Isot* **48**, 587 (May, 1997).
14. I. F. Tannock, D. Rotin, *Cancer Res* **49**, 4373 (Aug 15, 1989).